

# Catalyst FeNi supported on nanometric mezoporous oxide for PEMFC applications

E. C. SERBAN, N. BANU, A. C. MARINESCU, A. M. I. TREFILOV, A. ANDRONIE-BALAN, S. M. IORDACHE, A. CUCU, C. CEAUS, O. CINTEZA<sup>a</sup>, S. STAMATIN<sup>b</sup>, I. STAMATIN\*

*University of Bucharest, Faculty of Physics, 3Nano-SAE Research Centre, P.O. Box MG-38, 077125 Magurele, Bucharest-Romania*

*<sup>a</sup>University of Bucharest, Physical Chemistry Department, Bucharest, Romania*

*<sup>b</sup>University of Southern Denmark, Campusvej 55, DK-5230 Odense, Denmark*

Proton exchange membrane fuel cells (PEMFC) are studied intensive for hydrogen – oxygen couple conversion into electrical power via electro-chemical process. Electrocatalyst performances (defined by specific area and catalytic activity) represent a key point for hydrogen oxidation – anode reaction. Pt is a representative catalyst in these applications, but it has a few drawbacks, such as CO poisoning. The present work is focused on the study of catalytic activity of nanometric Iron (Fe) - Nickel (Ni) couple deposited on TiO<sub>2</sub> / SiO<sub>2</sub> materials.

(Received October 24, 2011; accepted November 23, 2011)

*Keywords:* PEMFC, FeNi catalyst, TiO<sub>2</sub>/SiO<sub>2</sub>, Sol-gel

## 1. Introduction

Fuel cells are today recognized as the most clean power sources due to the direct conversion of the chemical energy in electricity and heat. They are the key components in the energy strategy and continuous advances in the fuel cells technology is underpinned on intensive research in field [1]. Proton exchange membrane fuel cells (PEMFCs) are the most promising candidates for a clean power source for electric vehicles or combustion engines in automotive transport due to its high energy-conservation efficiency, the possibility of using regenerative fuels, low or nonexistent emission levels of noxious or environmental pollutants, low operating temperature and relatively quick start-up [2,3]. The features that make PEMFC superior to other fuel cell types are low operation temperature and high voltage output [4]. What is remarkable is that cell voltage improvements have been accomplished by reducing platinum catalyst loadings. This expensive metal is commonly used to catalyze the sluggish oxygen reduction reaction in PEMFC [5]. The economic feasibility of PEMFCs is directly linked to further reductions of the precious platinum electrocatalyst and its poisoning to CO [4-7]. In this respect, researches have focused on high proton conduction (>100 mS/cm) at operation conditions 150-200°C with low level of humidification, the electrocatalyst support and its coating on membrane for high current density at constant output voltage [2, 8]. Hydrogen oxidation (anode) and oxygen reduction (cathode) reactions take place at the interfaces membrane-electrocatalyst-gas diffusion layer (triple-phase boundary in the catalyst layer). The major drawback is the transfer of electron to a high electronic conductive gas diffusion layer and the proton to the hydrated membrane. At cathode site, the catalyst – gas diffusion form the second triple phase boundary where the oxygen, electron and proton are

reduced to water. Another drawback is related to the cathodic reaction which is more sluggish than the anodic reaction. Considering also Pt poisoning to CO when supported on nanocarbon particles [7-10], the design of new advanced materials for accomplishing these multiple functions is required. This study focuses on the replacement of platinum nanocarbon support with ionic conductive oxide with high affinity for hydroxyl groups to keep an optimum hydration level. FeNi alloys were coprecipitated during iron and nickel salt hydrolysis reaction. Moreover, the potential application of Fe/Ni alloy as electrocatalysts deposited on SiO<sub>2</sub>/TiO<sub>2</sub> support by sol-gel technique in a micelles solution is studied.

## 2. Experimental

### 2.1. Materials

Surfactant dioctyl sulfosuccinate sodium salt named Aerosol OT (98%), sodium acetate (99%) and ammonium was from Sigma-Aldrich. Solution of 1-butanol extrapure, chloroform and powders of FeCl<sub>3</sub> (99%) and NiCl<sub>2</sub> (98%) was purchased from Merck. TiO<sub>2</sub> (Photocatalyst Sol X 550)-Type Nano Technology from Titan PE Tehnologies. Sodium hydroxide and organic derivative vinyltrietoxisilane-VTES (98%) from Fluka.

### 2.2. Silica nanoparticles synthesis in surfactant micelles

The micelles were prepared by dissolving 0.22 g of Aerosol-OT surfactant and 400  $\mu$ L 1-butanol in 5 mL distilled water. 30  $\mu$ L of chloroform were added under continuous stirring until a transparent solution is formed. The

silica nanoparticles were obtained by the hydrolysis reaction of the organic silane derivative VTES in an alkaline environment: 50  $\mu\text{L}$  of VTES were added to the micellar system while stirring for 30 minutes. In order to initialize the silica polymerization process, 10  $\mu\text{L}$  of ammonium solution 33% was added. The obtained solution was left to mature under continuous stirring for 20 hours at room temperature. Aerosol-OT surfactant and the 1-butanol co-surfactant were removed by water dialysis through a cellulose membrane at 12-14 KDa for 50 hours. The dialyzed solution was filtered using a 0.2  $\mu\text{m}$  cellulose filter to obtain the silica nanoparticle solution.

## 2.2 FeNi catalyst deposition on $\text{SiO}_2$

54 mg of anhydrous  $\text{FeCl}_3$  for synthesis and 50 mg of  $\text{NiCl}_2$  were added in 20 mg of sodium acetate ( $\text{CH}_3\text{COONa}\cdot 3\text{H}_2\text{O}$ ) solution 50%. A homogeneous solution of Ni-Fe acetate was obtained. In second stage, the Ni-Fe acetate solution was mixed with the silica sol and heated to 70°C. Then a 3M sodium hydroxide solution was added by titration until the pH 11. The solution was then washed with 8 M ammonia solution and with deionised water for  $\text{Cl}^-$  ion removal. A dark brown powder was obtained after filtering the solution.

## 2.3. FeNi catalyst deposition on $\text{TiO}_2$ – anatase

The same method was used for obtaining the FeNi catalyst supported on  $\text{TiO}_2$ , replacing the silica sol with a  $\text{TiO}_2$  sol solution. The obtained solution was washed, filtered and cleaned. Materials obtained were used to prove the electrochemical activity of  $\text{SiO}_2$ , respectively  $\text{TiO}_2$  for the development of a catalyst like Fe/Ni.

## 3. Characterizations

The nanoparticle size distribution was investigated by NanoZetaSizer ZEN 3600 using a red laser at 633 nm in the range from 0.6 nm to 6  $\mu\text{m}$ . For the catalysts particle size distribution, an aqueous solution containing 0.1 mg/l sample was used. The solution was ultrasonated 10 minutes at ambient temperature in an ultrasonic bath. The powder morphology was determined using optical microscopy in reflectance (Optech –Optical Technology) at 40X resolution. The electrochemical behaviour of the catalysts was investigated by cyclic voltammetry with VoltaLab PGZ 301 using a three electrode system at ambient temperature in 1M  $\text{H}_2\text{SO}_4$  electrolyte solution. The auxiliary electrode was Pt (XM 140), while the reference electrode was SCE (XR-110, Radiometer Analytical). The working electrode (WE) was spectroscopic graphite with an active area of  $1\text{cm}^2$ . The samples were fixed on the working electrode by a mixture of Nafion (25  $\mu\text{L}$ ) and isopropyl alcohol (75  $\mu\text{L}$ ) and dried at 50 °C.

## 4. Results and discussions

### 4.1 Optical microscopy

The samples were investigated by reflectance microscopy. Optical microscopy reveals a typical structure of FeNi deposited on nanooxides. The images reveal a specific topography where FeNi alloy is continuous coated on silica nanoparticles (Fig. 1). In case of  $\text{TiO}_2$  the metallic nanoparticles are randomly precipitated in droplets (Fig. 2).

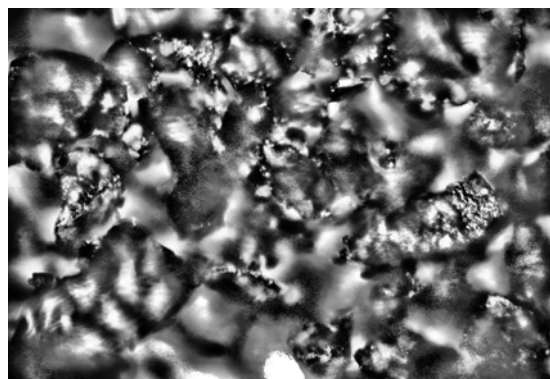


Fig. 1. Optical Microscopy (40X) - Catalyst FeNi deposited on the nanometric  $\text{SiO}_2$ .

### 4.2 Dimensional analysis

Fig. 3 represents the particle size distribution by number of FeNi/ $\text{TiO}_2$  with a mean value of 393.1 nm, and the particle size distribution by number of FeNi/ $\text{SiO}_2$  presented a mean value of 179.25 nm.

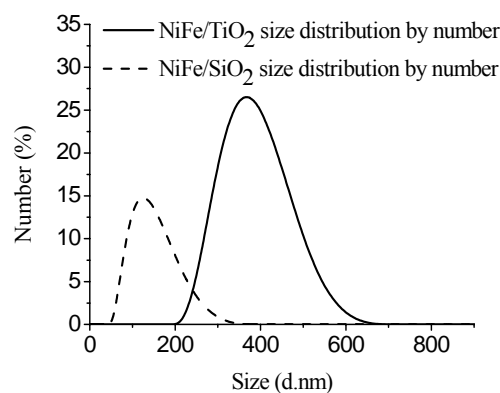


Fig. 3. The size distribution by number of FeNi/ $\text{TiO}_2$  with the mean value at 393.1nm and FeNi/ $\text{SiO}_2$  with a value at 179.25 nm.

### 4.3 The electrochemical characterization - CV:

The cyclic voltammograms of the catalysts were compared with and without  $\text{H}_2$  bubbling in the electrolyte solu-

tion. Well-defined voltammograms were obtained for both samples, before and after H<sub>2</sub> bubbling performed in the electrolyte solution [5].

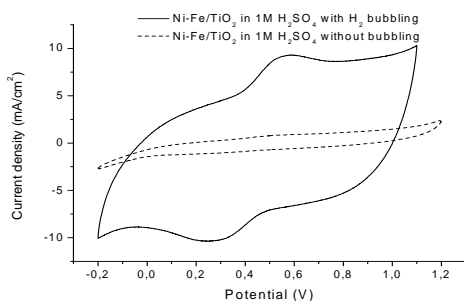


Fig. 4. The cyclic voltammograms of FeNi deposited on TiO<sub>2</sub> with/without H<sub>2</sub> bubbling.

In Figs. 4 and 5, FeNi/TiO<sub>2</sub> and respectively FeNi/SiO<sub>2</sub> samples have increased their efficient electrochemical surface once H<sub>2</sub> was bubbled inside the electrolyte solution. The samples in 1M H<sub>2</sub>SO<sub>4</sub> without H<sub>2</sub> bubbling, are showing a typical capacitive behavior presenting a very low current density [11-14]. The electrochemical activity of FeNi/TiO<sub>2</sub> sample, after 10 minutes of H<sub>2</sub> bubbling in the electrolyte solution, have shown two peaks related to the oxidation and reduction processes. The oxidation and reduction peaks have a value of 2.8 mA/cm<sup>2</sup> at a potential of E<sub>a</sub> = 549 mV respectively 2.23 mA/cm<sup>2</sup> at a potential of E<sub>c</sub> = 293 mV, ΔE = E<sub>a</sub> - E<sub>c</sub> = 256 mV which is higher than the value of 59 mV generally expected for a Nernstian behaviour for one electron transfer reaction. Also FeNi/SiO<sub>2</sub>, after H<sub>2</sub> bubbling in the electrolyte solution, shows an oxidation peak at the value of 3.08 mA/cm<sup>2</sup> with a potential of 498 mV and a reduction peak of 1.20 mA/cm<sup>2</sup> obtained at a potential of 352 mV. In this case, ΔE has a value of 146 mV. These samples bring out an electrochemical mechanism of reversible charge transfer preceded by electron transfer reaction [7, 8].

For both samples the total specific charge transfer Q<sub>T</sub> was calculated in the specific potential region:

$$Q_T = \frac{1}{\nu} \int_{E_i}^{E_f} (I_o - I_r) dE$$

Where ν is the sweep rate (100 mV/s), I<sub>o</sub> and I<sub>r</sub> are the current density for oxidation respectively reduction and E is the potential [13].

For the FeNi/TiO<sub>2</sub> sample, Q<sub>T</sub> has an estimated value of 1.67 mC/cm<sup>2</sup>, while for FeNi/SiO<sub>2</sub> Q<sub>T</sub> has a value of 3.69 mC/cm<sup>2</sup>.

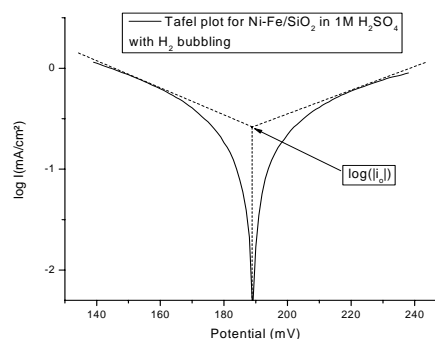


Fig. 6. Tafel plot for FeNi/SiO<sub>2</sub> in 1 M H<sub>2</sub>SO<sub>4</sub> with H<sub>2</sub> bubbling.

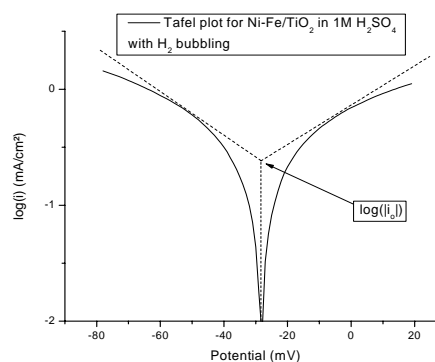


Fig. 7. Tafel plot for FeNi/TiO<sub>2</sub> in 1 M H<sub>2</sub>SO<sub>4</sub> with H<sub>2</sub> bubbling.

Figs. 6 and 7 are the Tafel plots for FeNi/SiO<sub>2</sub>, respectively FeNi/TiO<sub>2</sub>. The Tafel equation  $\eta = b \exp(i/i_0)$  gives the overpotential – current density relationship. This equation is revealing two main parameters in fuel cell catalysts, on one hand the exchange current density, *i*<sub>0</sub> and on the other hand the Tafel slope, *b* [8]. The specific values are presented in Table 1.

Table 1. Tafel parameters for FeNi/SiO<sub>2</sub> and FeNi/TiO<sub>2</sub>.

Sample	Over-potential (mV)	<i>i</i> <sub>0</sub> (μA/cm <sup>2</sup> )	<i>b</i> (mV)	Q <sub>T</sub> (mC/cm <sup>2</sup> )	C <sub>d</sub> (mF/cm <sup>2</sup> )
FeNi/SiO <sub>2</sub>	189	270	91.3	3.69	0.072
FeNi/TiO <sub>2</sub>	28.3	290	76.9	1.67	0.140
Pt	N/A	2570	25	N/A	N/A

The catalyst supported on SiO<sub>2</sub> has higher value for the Tafel slope, which is often translated into a higher overpotential value, which is confirmed by the second column. The exchange current density is an index for elec-

trocatalytic activity, this being much smaller comparable to Pt [13].

In conclusion the samples are displaying an electrochemical mechanism of charge transfer with a slow electron transfer.

## 5. Conclusions

The present study has investigated the electrochemical activity of FeNi deposited by chemical reduction mechanisms on two different support materials (nanooxide of Titanium/Silica).

The particle size distribution of FeNi/TiO<sub>2</sub> was of 393nm, while for FeNi/SiO<sub>2</sub> was 79nm. In the future the sizes of this particle have to be in the 10-20 nm range, in order to have a better catalytic activity.

The cyclic voltammetry measurements showed that both catalysts have a good response in the electrolyte solution with H<sub>2</sub> bubbling. The FeNi/SiO<sub>2</sub> catalysts has a better electrocatalytic activity, having a total specific charge transfer of 3.69 mC/cm<sup>2</sup> while FeNi/TiO<sub>2</sub> has a total specific charge transfer of 1.67mC/cm<sup>2</sup>, due to their particle size distribution.

The Tafel parameters reveal a good behaviour for the hydrogen oxidation reaction [14]. Even though, comparable to Pt, the exchange current density is smaller, it is expected to increase with a better nanooxide support. Also, the Tafel slope has a higher value comparable to Pt, which is translated to a higher overpotential value.

All in all, the samples investigated for the hydrogen oxidation reaction are being considered as a future catalyst for the anode reaction in PEM fuel cells. With an improved nanostructure as catalytic support, the catalysts are expected to behave in a much better manner.

## Acknowledgements

The authors acknowledge the financial support from national projects National Program PN-II, 22-136/2008, PN-II-ID-PCE-2011-3-0815.

## References

- [1] a) International Energy Agency (IEA), Fuel Cells, IEA Technology Essentials, Paris, OECD, 2007; b) Annual Progress Report, US. Department of Energy 2010.
- [2] S. Thomas, M. Zalbowitz, Fuel Cells- Green Power, Los Alamos, New Mexico 7-14, (2007).
- [3] G. Hoogers, Fuel Cell Technology Handbook, Boca Raton, FA: CRC Press 13-17, (2002).
- [4] P. Costamagna, S. Srinivasan, J. Power Sources **102**, 242 (2001).
- [5] H. A. Gasteiger, J. E. Panels, S. G. Yan, J. Power Sources, **127**, 162 (2004).
- [6] T. R. Ralph, G. A. Hards, J. E. Keating, S. A. Campbell, D. P. Wilkinson, M. Davis, J. St-Pierre, M. C. Johnson, J. Electrochem. Soc. **144**, 3845 (1997).
- [7] A. Guha, W. Lu, T. A. Zawodzinski Jr., D. A. Schiraldi, Carbon **45**, 1506 (2007).
- [8] F. Barbir, PEM Fuel Cells: Theory and Practice. Elsevier Academic Press, Burlington, MA., 39-45 (2005).
- [9] C. H. Hamann, A. Hamnett, W. Vielstich, Electrochemistry Wiley-VCH: New York, xvii, **423**, 121 (1998).
- [10] C. Lamy, J. M. Leger, S. Srinivasan, in: J. O'M. Bockris, B. E. Conway, R. E. White (Eds.), Modern Aspects of Electrochemistry, **34**, 53 (2001).
- [11] Chien-Te Hsieh, Yun-Wen Choua, Wei-Yu Chena, Journal of Alloys and Compounds **466**, 233 (2008).
- [12] Chien-Chung Chen, Chia-Fu Chen, I-Hsuan Lee, Chien-Liang Lin, Diamond & Related Materials **14**, 1897 (2005).
- [13] C. Song, Y. Tang, J. L. Zhang, J. Zhang, PEM fuel cell reaction kinetics in the temperature range of 23–120°C. Electrochim Acta **52**(7), 2552 (2007).
- [14] A. J. Appleby, H. Kita, M. Chemla, G. Bronoel, Hydrogen. In: Encyclopedia of the electrochemistry of the elements IXa. Bard A.J, editor. New York: Marcel Dekker 383 (1982).

\*Corresponding author: office@3nanosae.org